# Neutron-neutron intensity interferometry in $E/A=45$ MeV $^{58}$Ni+ $^{27}$Al, $^{nat}$Ni, and $^{197}$Au reactions

R. Ghetti,[1] N. Colonna,[2] B. Jakobsson,[1] J. Helgesson,[3] J. Mårtensson,[1] E. De Filippo,[4,5] G. Tagliente,[2] G. Lanzanò,[4,5] A. Pantaleo,[2] V. Bellini,[5,6] A. Anzalone,[6] S. Cavallaro,[5,6] L. Celano,[2] G. D'Erasmo,[2] D. Di Santo,[2] E. M. Fiore,[2] M. Geraci,[4] F. Giustolisi,[4,5] A. Kuznetsov,[7] D. Mahboub,[6] F. Merchez,[8] M. Palomba,[2] V. Paticchio,[2] G. Riera,[6] M. L. Sperduto,[5,6] C. Sutera,[4,5] and M. Urrata[6]

(CHIC Collaboration)

[1]*Department of Physics, Lund University, Box 118, SE-221 00 Lund, Sweden*
[2]*INFN and Dipartimento di Fisica, V. Amendola 173, I-70126 Bari, Italy*
[3]*Malmö University, SE-205 06 Malmö, Sweden*
[4]*INFN, Sezione di Catania, Corso Italia 57, I-95129 Catania, Italy*
[5]*Dipartimento di Fisica, Università di Catania, Corso Italia 57, I-95129 Catania, Italy*
[6]*Laboratori Nazionali del Sud (INFN), Via S. Sofia 44, I-95123 Catania, Italy*
[7]*Khlopin Radium Institute, Shvernik av. 28, 194021 St. Petersburg, Russia*
[8]*Institut des Sciences Nucléaires, F-38026 Grenoble, France*

(Received 19 April 2000; published 14 August 2000)

Small angle neutron-neutron correlations have been measured for the $E/A=45$ MeV $^{58}$Ni+ $^{27}$Al, $^{nat}$Ni, and $^{197}$Au reactions. Two-neutron correlation functions, both integrated and gated on the total momentum of the neutron pair, have been constructed. In order to explain these data, a fraction of fast ''dynamical'' emission is needed in addition to slower evaporative emission. The overall emission time scale is shorter for the symmetric system, indicating that the dynamical component is stronger in this case.

PACS number(s): 25.70.Pq, 29.30.Hs

Over the past three decades, two-particle intensity interferometry has been extensively utilized to determine the space-time extension of particle emitting sources in nuclear and particle physics [1–4]. To this end, the CHIC Collaboration has undertaken a program of fermion interferometry [5] in which quantum statistical and final state effects are singled out by simultaneous measurements of neutron-neutron ($nn$), neutron-proton ($np$), and proton-proton ($pp$) correlation functions [6–10]. Within this program, an experimental investigation of 45$A$ MeV $^{58}$Ni-induced reactions has recently been performed at the superconducting cyclotron of Laboratori Nazionali del Sud (LNS) in Catania. In this experiment, single-particle kinetic energy spectra as well as $nn$, $pp$, and $np$ small-angle correlations were measured in coincidence with forward-emitted fragments.

The experimental setup and results for the $^{58}$Ni+ $^{27}$Al reaction have been presented in some detail elsewhere [9,10]. From simultaneous fits to $n$ and $p$ single-particle energy spectra and to $nn$, $pp$, and $np$ correlation functions calculated with the statistical model of Ref. [11], the neutron and proton emitting sources have been characterized in terms of global parameters such as Gaussian radius, exponential lifetime, initial temperature, source velocity, and flow velocity. In this Brief Report we introduce $n$ spectra and $nn$ correlations for two additional reactions $^{58}$Ni+ $^{nat}$Ni and $^{58}$Ni + $^{197}$Au (45$A$ MeV). The energy spectra are fitted to Maxwell-Boltzmann distributions in order to extract velocity and temperature parameters for the emission sources. Both integrated neutron-neutron correlation functions and correlation functions gated on the total momentum of the neutron pairs are presented.

Figure 1 presents the efficiency-corrected singles neutron kinetic energy distributions measured at 25°, 45°, and 90° for the $^{58}$Ni+ $^{27}$Al (upper panel), $^{58}$Ni+ $^{nat}$Ni (middle panel), and $^{58}$Ni+ $^{197}$Au (lower panel) reactions, together with Maxwell-Boltzmann fits (solid lines). The distributions are shown only up to $E=50$ MeV since the contamination from protons passing through the detector container walls created severe distortions in the spectra at $E>50$ MeV.[1] The statistical errors are smaller than the symbols. The systematic errors (not shown) extend up to 20% due to the efficiency correction. The neutron energy spectra show a Boltzmann-like shape shifted by the source velocity in the laboratory frame. Temperature ($T_{slope}$) and source velocity ($v_{source}$) parameters have been extracted by fitting a Galilei-transformed Maxwellian source (for volume emission):

$$\frac{d^2\sigma}{dEd\Omega}=\text{const}\times\sqrt{E}\exp\left(-\frac{E+E_0-2\sqrt{EE_0}\cos\theta}{T_{slope}}\right), \quad (1)$$

where $E_0=\frac{1}{2}mv_{source}^2$ and $E$ and $\theta$ are the kinetic energy and neutron emission angle in the laboratory frame. The temperature $T_{slope}$ has been fixed by fitting Eq. (1) to the 90° spectrum while the 25° and 45° spectra provide individual velocity parameters (see Table I). For reference, Table I presents also the values of source velocity ($v_{\text{c.m.}}$) and temperature ($T_{Fermi}=\sqrt{E^*/a}$, $a=A/8$, $E^*=$ excitation energy) calculated within the assumption of total fusion. The temperatures extracted for $^{58}$Ni+ $^{27}$Al and $^{58}$Ni+ $^{197}$Au are quite close to

[1]As discussed in Ref. [9], the proton contamination of the high-energy tail of the neutron spectra does not affect the $nn$ correlation functions, in particular after the application of the cross talk rejection condition.

 

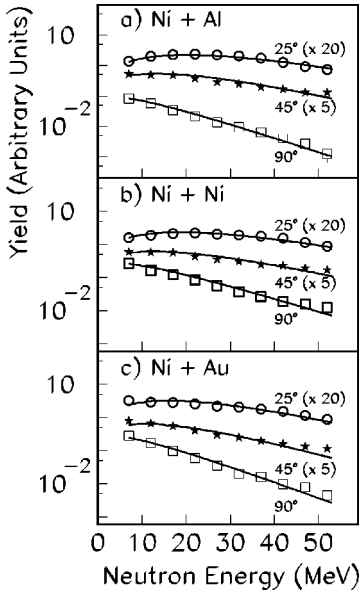


FIG. 1. Neutron kinetic energy distributions (corrected for detection efficiency) from 45*A* MeV: (a)$^{58}$Ni+ $^{27}$Al, (b) $^{58}$Ni+$^{\text{nat}}$Ni, and (c) $^{58}$Ni+ $^{197}$Au collisions, at 25° (circles), 45° (stars), and 90° (squares) in the laboratory frame. The 90° distributions are arbitrarily normalized; the 25° and 45° distributions are normalized to 5 times and 20 times relative to the normalization of the 90° distribution, respectively. The systematic uncertainty (not shown in the figure) is estimated to ~20%. The solid lines are Maxwell-Boltzmann fits (see text).

each other and are both lower than the temperature for the symmetric $^{58}$Ni+$^{\text{nat}}$Ni collision. The reverse kinematics $^{58}$Ni+ $^{27}$Al reaction exhibits a source velocity slightly lower than the center-of-mass velocity. In contrast, the $^{58}$Ni + $^{197}$Au reaction exhibits a velocity significantly higher than the center-of-mass one. The lower source velocities measured at 45° as compared to 25° are probably connected to the different degree of centrality of the collisions selected at different polar angles. Some deviations between data and the Maxwellian one-source fits for the highest neutron energies (seen in Fig. 1) do show that this is an oversimplified picture and that a multisource fit [12,13] would naturally improve the agreement.

Experimentally the correlation function is constructed by dividing the coincidence yield $N_c$ by the yield for uncorrelated events $N_{nc}$:

TABLE I. Temperature ($T_{slope}$) and source velocity ($v_{source}$) parameters extracted from the Maxwell-Boltzmann fits to the angle-gated neutron kinetic energy distributions. The parameters $E^*$, $T_{Fermi}$, and $v_{\text{c.m.}}$ are calculated within the assumption of total fusion.

| Target | $E^*/A$ (MeV) | $T_{Fermi}$ (MeV) | $T_{slope}$ (MeV) | $v_{\text{c.m.}}/c$ | $v_{source}/c$ 25° | $v_{source}/c$ 45° |
|---|---|---|---|---|---|---|
| $^{27}$Al | 9.7 | 8.8 | 8.5±1.5 | 0.20 | 0.18±0.02 | 0.16±0.02 |
| $^{\text{nat}}$Ni | 11.2 | 9.4 | 10±1.5 | 0.15 | 0.16±0.02 | 0.14±0.02 |
| $^{197}$Au | 7.9 | 7.9 | 8.0±1.5 | 0.07 | 0.15±0.02 | 0.13±0.02 |

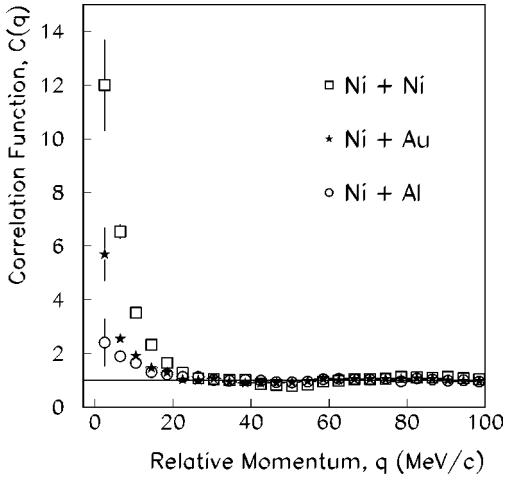


FIG. 2. Cross-talk-corrected and background-rejected neutron-neutron correlation functions for $^{58}$Ni+ $^{27}$Al (circles), $^{58}$Ni+$^{\text{nat}}$Ni (squares), and $^{58}$Ni+ $^{197}$Au (stars). All background yields have been generated from the product of singles distributions and independent normalization constants have been calculated constraining each correlation function to go to unity in the region $40<q<100$ MeV/$c$. The error bars in $C(q)$ represent statistical errors. The uncertainty in $q$ falls within the symbol size.

$$C(\vec{q},\vec{P}_{tot}) = K\frac{N_c(\vec{q},\vec{P}_{tot})}{N_{nc}(\vec{q},\vec{P}_{tot})}. \tag{2}$$

In the above expression, the relative momentum $\vec{q}=(\vec{p}_1-\vec{p}_2)/2$ and the total momentum $\vec{P}_{tot}=\vec{p}_1+\vec{p}_2$ of the particle pair are introduced. The normalization constant $K$ is determined so that the correlation function goes to unity at large values of $q$, where no correlations are expected. Figure 2 shows the experimental $^{58}$Ni+ $^{27}$Al (circles), $^{58}$Ni+$^{\text{nat}}$Ni (squares), and $^{58}$Ni+ $^{197}$Au (stars) neutron-neutron correlation functions obtained from all four clusters of neutron detectors in our experimental setup.[2] The denominator is constructed with the ''singles-product'' technique [9,14] and the correlation functions are normalized in the region $40<q<100$ MeV/$c$. The correlation functions are corrected for cross talk between neighboring detectors [9,14,15] and background suppressed [9]. Furthermore, the data are sorted with the ''minimum bias'' requirement that at least one fragment ($Z>1$) is detected in the two inner rings of the forward wall [9], in coincidence with the neutron pair.

The large difference in strength of the three correlation functions probes the time scale of the reactions. In particular, the fact that the smallest system has the weakest correlation indicates that the time scale for the $^{58}$Ni+ $^{27}$Al collision, estimated to $\approx 600\pm 200$ fm/$c$ (exponential lifetime for neutron emission) in [10], must be the largest one. The fact that the $^{58}$Ni+$^{\text{nat}}$Ni correlation function exhibits the largest strength is expected, due to the high excitation energy per

[2]Six liquid scintillators of the 25° cluster were switched off in the off-line analysis of the $^{58}$Ni+$^{\text{nat}}$Ni reaction, due to the large background of scattered particles.

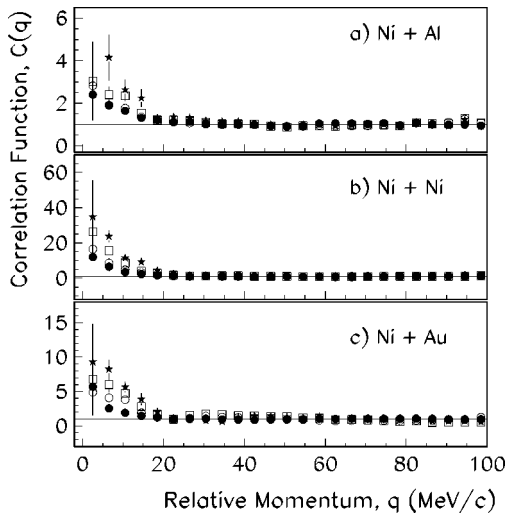


FIG. 3. High-total-momentum gated *nn* correlation functions are compared to the ungated ones (solid circles). The total momentum of the *nn* pair is calculated in the reference frame of a source moving with (a) $v_s/c=0.17$, (b) $v_s/c=0.15$, and (c) $v_s/c=0.14$. The high-total-momentum gates correspond to $P_{tot}>180$ MeV/$c$ (open circles), $P_{tot}>210$ MeV/$c$ (squares), and $P_{tot}>240$ MeV/$c$ (stars). All background yields have been generated from the product of singles distributions and independent normalization constants have been calculated, constraining each correlation function to go to unity in the region $40<q<100$ MeV/$c$.

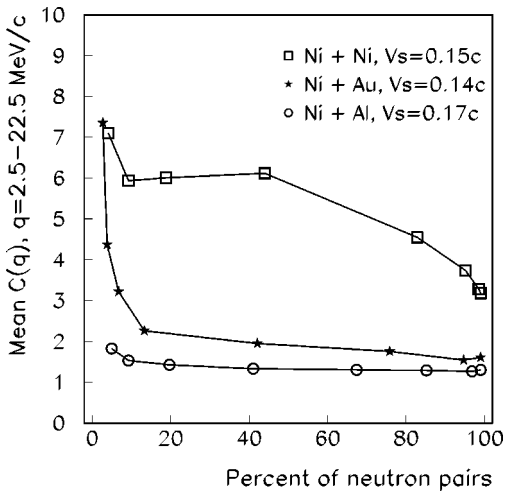


FIG. 4. The strength of the correlation function (weighted in the small relative momentum region $q=2.5$–$22.5$ MeV/$c$) is plotted as a function of the fraction of high-total-momentum neutron pairs selected by the successive $P_{tot}$ gates applied to the neutron coincidence yield. The total momentum distributions of the neutron pairs are cross talk rejected and are calculated in the reference frame of a source moving with $v_{\mathrm{c.m.}}/c=0.17$ for $^{58}$Ni+ $^{27}$Al (circles), $v_{\mathrm{c.m.}}/c=0.15$ for $^{58}$Ni+$^{\mathrm{nat}}$Ni (squares), and $v_{\mathrm{c.m.}}/c=0.14$ for $^{58}$Ni + $^{197}$Au (stars).

nucleon of this symmetric system. On the other hand, the larger strength of $^{58}$Ni+ $^{197}$Au as compared to $^{58}$Ni+ $^{27}$Al is unexpected and not easily explained as the excitation energy per nucleon for a central collision is larger in the latter reaction. A possible explanation that can be put forward in light of recent experimental findings [12,13,16–18] is that of ''dynamical'' neutron emission from a highly excited fireball-like source created in the overlap region. This ''midvelocity'' emission, as opposite to the slow statistical evaporative processes from the quasiprojectile and quasitarget sources, is thought to be influenced by dynamical effects (including preequilibrium and neck emission [19]) and to proceed on a relatively short time scale. As expected from geometrical considerations, the importance of this ''midvelocity'' source should increase with system size, thus explaining the larger correlation function strength of $^{58}$Ni+$^{\mathrm{nat}}$Ni as compared to $^{58}$Ni+ $^{27}$Al. The smaller strength observed in $^{58}$Ni+ $^{197}$Au as compared to $^{58}$Ni+$^{\mathrm{nat}}$Ni would instead be due to less available energy per nucleon.

In order to get further insight into the time scale and source shape of the reactions, we have investigated the directional dependence of the two-particle correlation function on the angle $\psi=\cos^{-1}(\vec{P}_{tot}\cdot\vec{q})/(P_{tot}q)$ defined in the rest frame of the emitting system. A long-lived source should exhibit an enhancement of the longitudinal ($\vec{q}\|\vec{P}_{tot}$) correlation function due to the stronger Pauli anticorrelation in the transverse direction [20,21]. Apart from a very small effect observed for the $^{58}$Ni+ $^{27}$Al system, we find that the longitudinal correlation functions (constructed by gating on $\psi\leqslant 50°$ and properly normalized using the same normalization constant as for the ungated correlation function [22]) do not exhibit a significative enhancement as compared to the ungated ones (the results are not shown in this Brief Report). This stresses that the long-time part of the emission does not seem to be responsible for the large difference in the strength of the integrated correlation functions.

A complementary way to investigate the time scale of the emission and to study the interplay between dynamical and statistical effects in the particle emission is to gate the correlation function on the momentum (or energy) of the particle pair [9,10]. In particular, the preequilibrium emission [6,8,17,23–25] could be probed by high-momentum pairs. Figure 3 compares high-total-momentum gated *nn* correlation functions with the ungated ones (solid circles). The strength increases systematically when the cut is made at higher values of $P_{tot}$, indicating a reduction in the time scale for the emission of the more energetic particles. One can note that the correlation function can reach quite high values for strong $P_{tot}$ cuts (particularly for Ni+Ni), due to the fact that mainly particles emitted close in time and space are selected. This behavior agrees qualitatively with the results of theoretical calculations performed for the $^{58}$Ni+ $^{27}$Al reaction [9]. The calculations indicated that, although the $^{58}$Ni+ $^{27}$Al reaction is dominated by low-energy evaporated neutrons, a non-negligible preequilibrium component is needed to reproduce the enhanced correlation observed when a cut on high-total-momentum neutron pairs is applied [9,10]. However, the very different strength of the $P_{tot}$-cut enhancement seen for the $^{58}$Ni+$^{\mathrm{nat}}$Ni system in Fig. 3 (note the very different scale on the *y* axis) indicates that the symmetric system is much more affected by ''dynamical'' emission than the asymmetric ones.

The latter statement is illustrated Fig. 4, where we have plotted the height of the correlation function (weighted in the

$q$ region 2.5–22.5 MeV/$c$) versus the fraction of neutron pairs selected by gates of increasing total momentum applied to the neutron coincidence yield. One can notice that for the asymmetric $^{58}$Ni+ $^{27}$Al and $^{58}$Ni+ $^{197}$Au reactions, the increase of the correlation function strength becomes significant only when the applied cut selects neutron pairs on the very tail of the total momentum distribution ($<20\%$ of the total yield). For the symmetric $^{58}$Ni+$^{nat}$Ni system, instead, the correlation function strength increases continuously when selecting more and more energetic pairs. The behavior observed in Fig. 4 is easily interpreted within the ''midvelocity'' emission picture mentioned above. While for the asymmetric systems either projectilelike or targetlike emission is dominating and only a very small fraction of the highly energetic pairs is coming from the ''midvelocity'' source, in the $^{58}$Ni+$^{nat}$Ni case the ''midvelocity'' source is always present (even dominant). This seems to be in agreement with the very recent experimental findings reported in Ref. [16], concerning the onset of ''midvelocity'' emission in symmetric systems at intermediate energies.

In summary, two-neutron correlation functions from $E/A=45$ MeV $^{58}$Ni+ $^{27}$Al, $^{nat}$Ni, and $^{197}$Au reactions, integrated as well as gated on the direction of emission and on the total momentum of the neutron pair, have been measured. The overall neutron emission time scale is shorter for the symmetric system. Even so, also the data on asymmetric reactions need some fraction of fast emission to be explained. The different correlation strength for the different systems suggests that an important contribution to neutron emission might be coming from a hot, fireball-like ''midvelocity'' source created in the overlap region. Furthermore, a comparison of the momentum gated correlation functions for the different systems indicates that the relative importance of the various sources depends strongly on the degree of mass asymmetry of the reaction.

The authors wish to thank G. Antuofermo, G. Iacobelli, M. Sacchetti, P. Vasta, A. Masciullo, G. Poli, N. Guardone, and V. Sparti for technical support and the LNS accelerator crew for providing a high-quality pulsed beam. Financial support from the ''Knut och Alice Wallenberg'' and ''Helmuth Hertz'' Foundations is gratefully acknowledged by R.G. Support from the Swedish Natural Science Research Council is appreciated.

[1] D. H. Boal, C. K. Gelbke, and B. K. Jennings, Rev. Mod. Phys. **62**, 553 (1990).
[2] D. Ardouin, Int. J. Mod. Phys. E **6**, 391 (1997).
[3] P. A. DeYoung *et al.*, Nucl. Phys. **A597**, 127 (1996).
[4] S. J. Gaff *et al.*, Phys. Rev. C **58**, 2161 (1998).
[5] S. E. Koonin, Phys. Lett. **70B**, 43 (1977).
[6] B. Jakobsson *et al.*, Phys. Rev. C **44**, 1238 (1991).
[7] R. Ghetti, L. Carlén, M. Cronqvist, B. Jakobsson, F. Merchez, B. Norén, D. Rebreyend, M. Rydehell, Ö. Skeppstedt, and L. Westerberg, Nucl. Instrum. Methods Phys. Res. A **335**, 156 (1993).
[8] M. Cronqvist *et al.*, Phys. Lett. B **317**, 505 (1993).
[9] R. Ghetti *et al.*, Nucl. Phys. **A660**, 20 (1999).
[10] R. Ghetti *et al.*, Nucl. Phys. **A674**, 277 (2000).
[11] J. Helgesson, T. Csörgo, M. Asakawa, and B. Lörstad, Phys. Rev. C **56**, 2626 (1997).
[12] Y. Larochelle *et al.*, Phys. Rev. C **59**, R565 (1999).
[13] G. Lanzanò *et al.*, Phys. Rev. C **58**, 281 (1998).
[14] R. Ghetti, N. Colonna, and J. Helgesson, Nucl. Instrum. Methods Phys. Res. A **421**, 542 (1999).
[15] N. Colonna *et al.*, Nucl. Instrum. Methods Phys. Res. A **381**, 472 (1996).
[16] The INDRA Collaboration, E. Plagnol *et al.*, Phys. Rev. C **61**, 014606 (1999).
[17] Ph. Eudes, Z. Basrak, and F. Sébille, Phys. Rev. C **56**, 2003 (1997).
[18] P. A. DeYoung *et al.*, Phys. Rev. C **56**, 244 (1997).
[19] M. Colonna, M. Di Toro, and A. Guarnera, Nucl. Phys. **A589**, 160 (1995); M. Colonna, M. Di Toro, A. Guarnera, V. Latora, A. Smerzi, and Z. Jiquan, Nucl. Phys. **A583**, 525c (1995).
[20] S. Pratt and M. B. Tsang, Phys. Rev. C **36**, 2390 (1987).
[21] N. Colonna, D. R. Bowman, L. Celano, G. D'Erasmo, E. M. Fiore, L. Fiore, A. Pantaleo, V. Paticchio, G. Tagliente, and S. Pratt, Phys. Rev. Lett. **75**, 4190 (1995).
[22] W. G. Gong *et al.*, Phys. Rev. C **43**, 1804 (1991).
[23] D. Ardouin, P. Lautridou, D. Durand, D. Goujdami, F. Guibault, C. Lebrun, A. Peghaire, J. Quebert, and F. Saint-Laurent, Nucl. Phys. **A465**, 57c (1989).
[24] W. G. Gong *et al.*, Phys. Rev. C **47**, R429 (1993).
[25] D. O. Handzy *et al.*, Phys. Rev. Lett. **75**, 2916 (1995).